

1 Branching and intercellular communication in the Section V cyanobacterium

2 *Mastigocladus laminosus*, a complex multicellular prokaryote

3 Dennis J Nürnberg<sup>1</sup>, Vicente Mariscal<sup>2</sup>, Jamie Parker<sup>1</sup>, Giulia Mastroianni<sup>1</sup>, Enrique Flores<sup>2</sup>, and

4 Conrad W Mullineaux<sup>1#</sup>

5 <sup>1</sup>School of Biological and Chemical Sciences, Queen Mary University of London, Mile End

6 Road, London E1 4NS, United Kingdom

7 <sup>2</sup>Instituto de Bioquímica Vegetal y Fotosíntesis, Consejo Superior de Investigaciones Científicas

8 and Universidad de Sevilla, Américo Vespucio 49, E-41092 Seville, Spain

9 # For correspondence. E-mail c.mullineaux@qmul.ac.uk; Tel. (+44) 20 7882 3645; Fax (+44) 20

10 8983 0973.

11 Running title: Intercellular communication in *Mastigocladus laminosus*

12 Keywords: cyanobacteria, true branching, *Mastigocladus laminosus*, intercellular

13 communication, SepJ, cell differentiation

---

This article has been accepted for publication and undergone full peer review but has not been through the copyediting, typesetting, pagination and proofreading process, which may lead to differences between this version and the Version of Record. Please cite this article as doi: 10.1111/mmi.12506

## 14 Summary

15 The filamentous Section V cyanobacterium *Mastigocladus laminosus* is one of the most  
16 morphologically complex prokaryotes. It exhibits cellular division in multiple planes, resulting in  
17 the formation of true branches, and cell differentiation into heterocysts, hormogonia and necridia.  
18 Here, we investigate branch formation and intercellular communication in *M. laminosus*.  
19 Monitoring of membrane rearrangement suggests that branch formation results from a  
20 randomised direction of cell growth. Transmission electron microscopy reveals cell junction  
21 structures likely to be involved in intercellular communication. We identify a *sepJ* gene, coding  
22 for a potential key protein in intercellular communication, and show that SepJ is localised at the  
23 septa. To directly investigate intercellular communication, we loaded the fluorescent tracer 5-  
24 carboxyfluorescein diacetate into the cytoplasm, and quantified its intercellular exchange by  
25 Fluorescence Recovery after Photobleaching. Results demonstrate connectivity of the main  
26 trichome and branches, enabling molecular exchange throughout the filament network. Necridia  
27 formation inhibits further molecular exchange, determining the fate of a branch likely to become  
28 a hormogonium. Cells in young, narrow trichomes and hormogonia exhibited faster exchange  
29 rates than cells in older, wider trichomes. Signal transduction to coordinate movement of  
30 hormogonia might be accelerated by reducing cell volume.

## 31 Introduction

32 Among non-eukaryotes, cyanobacteria have achieved a high degree of morphological complexity  
33 and diversity. It is remarkable that multicellularity in this phylum evolved early in Earth history,  
34 possibly as early as the “Great Oxygenation Event” that took place around 2.48 to 2.32 billion  
35 years ago and allowed the development of all life we know today (Bekker *et al.*, 2004; Tomitani

36 *et al.*, 2006; Konhauser *et al.*, 2011; Schirmer *et al.*, 2011). According to their morphology,  
37 cyanobacteria have been divided into five sections, including unicellular forms (Section I and II),  
38 filamentous (Section III and IV) and filamentous-branching forms (Section V) (Rippka *et al.*,  
39 1979). Organisms of Section IV (also known as order Nostocales (Komárek and Anagnostidis,  
40 1989)) and V (Stigonematales (Anagnostidis and Komárek, 1990)) show additionally the ability  
41 to undergo cell differentiation, forming heterocysts (specialised cells for nitrogen fixation), and  
42 sometimes also akinetes (resting cells for survival of adverse environmental conditions), and  
43 hormogonia (motile filaments for dispersal and symbiosis competence). Accordingly,  
44 multicellularity in cyanobacteria has been defined by three processes: cell-cell adhesion,  
45 intercellular communication and terminal cell differentiation (Flores and Herrero, 2010).

46 While our understanding of multicellularity in Section IV has deepened considerably by studying  
47 *Anabaena* sp. PCC 7120 as model organism (for review see (Flores and Herrero, 2010)), there is  
48 little known about cyanobacteria of Section V. The best understood organism within this section  
49 is probably *Mastigocladus laminosus*, which is a major component of epilithic microbial mats at  
50 White Creek, Yellowstone National Park, USA (Miller *et al.*, 2006), and can be found in  
51 geothermal sites and hot springs worldwide with an upper temperature limit of 63°C (Cohn,  
52 1862; Schwabe, 1960; Castenholz, 1976; Melick *et al.*, 1991; Finsinger *et al.*, 2008; Soe *et al.*,  
53 2011; Mackenzie *et al.*, 2013).

54 Under most conditions, *M. laminosus* forms a dense network of intertwined narrow and wide  
55 trichomes (also known as type II (secondary) and type I (primary) trichomes respectively  
56 (Schwabe, 1960)). While cells of narrow trichomes have a uniform cylindrical shape, cells of  
57 wide trichomes are rounded and pleomorphic, giving usually rise to true branches, the  
58 characteristic feature for cyanobacteria of Section V (Anagnostidis and Komárek, 1990; Golubić

59 *et al.*, 1996; Komárek *et al.*, 2003). Microfossil records from Rhynie, Aberdeenshire, Scotland  
60 support the presence of this complex morphotype already around 400 million years ago (Croft  
61 and George, 1959). True branching includes several different types, which have been named for  
62 simplicity after their morphological appearance, including “T”, “V”, “X”, and (reverse) “Y”  
63 branching (Anagnostidis and Komárek, 1990; Golubić *et al.*, 1996). Lateral “T”, “V” and  
64 (reverse) “Y” branches are comprised of cylindrical cells (Desikachary, 1959; Fogg *et al.*, 1973;  
65 Golubić *et al.*, 1996). Branches can differentiate into motile hormogonia which are released from  
66 the main filament by death and disintegration of the branching point (Balkwill *et al.*, 1984). The  
67 released hormogonia glide away from the parental colony, and finally form new colonies by  
68 differentiating into spherical cells, which give rise to new lateral branches (Hernandez-Muniz and  
69 Stevens, 1987; Robinson *et al.*, 2007). According to ultrastructural investigations, cell division in  
70 *M. laminosus* and *Fischerella ambigua* differs from that seen in filamentous cyanobacteria of  
71 Sections III and IV (Thurston and Ingram, 1971; Martin and Wyatt, 1974; Nierzwicki *et al.*,  
72 1982). Rounded cells in wide trichomes were suggested to be separated by their surrounding  
73 sheath (Martin and Wyatt, 1974). This would suggest that their filamentous character is only  
74 maintained by sheath material, so cyanobacteria of Section V may not represent the pinnacle of  
75 development among cyanobacteria but rather a primitive and basic form linking coccoid and  
76 filamentous forms (Martin and Wyatt, 1974). Under nitrogen deprivation almost every cell can  
77 differentiate into a heterocyst, following no regular spacing pattern, often forming multiple  
78 contiguous heterocysts in wide trichomes (MCH; sets of heterocysts, connected to each other  
79 without vegetative cells in between) (Nierzwicki-Bauer *et al.*, 1984a; Nierzwicki-Bauer *et al.*,  
80 1984b; Stevens *et al.*, 1985). This raises the question of how cells communicate in *M. laminosus*.  
81 Here we investigate intercellular communication in *M. laminosus* by loading the fluorescent  
82 tracer 5-carboxyfluorescein diacetate (5-CFDA) into the cytoplasm, and performing Fluorescence

83 Recovery after Photobleaching (FRAP) experiments to observe intercellular exchange of dye  
84 molecules, using methodology previously applied to filamentous cyanobacteria of Sections III  
85 and IV (Mullineaux *et al.*, 2008). In the Section IV cyanobacterium *Anabaena* sp. PCC7120,  
86 there is rapid diffusion of dye molecules between the cytoplasm of neighbouring cells,  
87 dependent on the septum-localised proteins SepJ (FraG), FraC and FraD (Mullineaux *et al.*, 2008;  
88 Merino-Puerto *et al.*, 2011). Here, we address the questions of whether the branch and the main  
89 trichome communicate in *M. laminosus*, and whether exchange depends on the cell morphotype.  
90 Our results demonstrate that branch and main trichome exchange molecules, and that exchange  
91 depends on the cell morphology, showing that *M. laminosus* makes a particularly complex  
92 network of intercellular communication.

93 Just recently, the genome sequences of several species of Section V were published (Dagan *et al.*,  
94 2013; Shih *et al.*, 2013). It has been suggested that no signature proteins specific to any of the  
95 complex morphologies exist (Shih *et al.*, 2013), and that branching might be mainly a result of  
96 expressing a very few proteins which affect the regulation of cell division genes and/or the  
97 localisation of their proteins (Dagan *et al.*, 2013). Here we follow the localisation of the  
98 cytoplasmic membrane during the process of branch formation to gain further insights into this  
99 complex event.

100

## 101 Results and Discussion

### 102 **Randomisation of the axis of growth results in different types of branching**

103 *M. laminosus* forms two morphologically distinct types of true branches: (reverse) “Y” (Fig. 1A)  
104 and “T” branches (Fig. 1B). Both types of branches are not only present in the same culture, but  
105 even in the same filament (not shown), raising the question of whether the differences between  
106 the two types are merely superficial, or whether they arise from different developmental  
107 processes.

108 We approached this question by visualising the cytoplasmic membrane during branch formation  
109 using confocal microscopy and transmission electron microscopy. For confocal microscopy we  
110 stained cells with the fluorescent dye FM1-43FX, which highlights the cytoplasmic membrane in  
111 cyanobacteria (Schneider *et al.*, 2007). Our results indicate that the (reverse) “Y” and “T”  
112 branches are topologically equivalent: in both cases branch formation is initiated by the growth of  
113 a cell in a direction other than the main axis of the filament (Fig. 1A,C). This is generally  
114 followed by septum formation across the mid-line of the cell, as is the usual rule in bacteria (Fig.  
115 1A). The result of septum formation is that one of the daughter cells is connected to three cells:  
116 two in the main trichome and one in the developing branch (Fig. 1A,B). A “T” branch results  
117 from cell elongation in a direction roughly perpendicular to the filament axis (Fig. 1B), whereas a  
118 (reverse) “Y” branch results from cell elongation at a more acute angle to the filament axis (Fig.  
119 1A,C), but the two cases are only superficially different. This implies that branching is the result  
120 of a randomisation of the direction of cell elongation. When cell elongation is constrained to  
121 occur along the filament axis, branch formation is repressed. A developmental switch leading to  
122 randomisation of the direction of cell elongation allows branches to form. Our conclusion is  
123 consistent with the message from recent genome sequence analyses of several cyanobacteria of

124 Section V, which did not detect any specific Section V signature proteins (Dagan *et al.*, 2013;  
125 Shih *et al.*, 2013). Furthermore, it was shown by Singh and Tiwari (1969) that true branching can  
126 be induced in the non-branching filamentous cyanobacterium *Nostoc linckia* (Roth) Born. et Flah.  
127 (Section IV) by random mutagenesis using ultraviolet irradiation, which implies that branching  
128 can be induced by loss of gene function rather than being the result of a complex developmental  
129 programme. This fits with our conclusion that branching results from the selective relaxation of a  
130 stringent control over the direction of cell elongation. We could detect no obvious patterns in the  
131 spacing of branches, which appears to be random. Terminal cells of wide trichomes do not branch  
132 and have a different, elongated shape (Fig. 1D), which has been described as a terminal hair  
133 (Anagnostidis and Komárek, 1990). The attachment of another cell, or even a cell fragment, at  
134 the terminus of the filament is enough to inhibit cell elongation (Fig. S1). A similar topology can  
135 be found e.g. in the filamentous cyanobacterium *Oscillatoria acuminata* (Section III; Geitler,  
136 1960).

137

### 138 ***M. laminosus* forms a complex cellular network of communication mediated by septosomes**

139 Until now it has remained unknown whether the branch and the main trichome communicate in  
140 cyanobacteria of Section V. A prerequisite for answering this question is to load a hydrophilic  
141 fluorescent molecule into the cytoplasm of cells of both the branch and the main trichome. For  
142 *Anabaena* sp. PCC 7120 two fluorescent molecules that can be used as tracers have been  
143 described in detail, calcein (Mullineaux *et al.*, 2008) and 5-carboxyfluorescein diacetate (5-  
144 CFDA; Mariscal *et al.*, 2011). In both cases, the tracer is added to the cell culture in an esterified  
145 form which is non-fluorescent and hydrophobic enough to be cell-permeant. Hydrolysis of the  
146 ester groups by cytoplasmic esterases converts the molecule to a fluorescent form which is

147 trapped in the cytoplasm because it is too hydrophilic to traverse lipid bilayers. Hence it can be  
148 used to probe intercellular exchange of hydrophilic molecules via protein channels at the cell  
149 junctions (Mullineaux *et al.*, 2008; Mariscal *et al.*, 2011). We tested both fluorescent tracers for  
150 *M. laminosus*. The efficiency of cell labelling with 5-CFDA was much higher than that with  
151 calcein (data not shown), and hence suitable for further studies.

152 The question of connectivity between branch and main trichome cannot be answered simply by  
153 photobleaching and following fluorescence recovery of the cell at the branch point, as  
154 fluorescence recovery might be possible from three directions. We found that branch formation  
155 could be induced by agitating the cell culture for 24h in fresh medium, consistent with a previous  
156 observation that branch formation is induced by conditions favouring rapid growth (Thurston and  
157 Ingram, 1971). Cells were then loaded with 5-CFDA, and fluorescence of entire short branches  
158 bleached by scanning the region of the branch at increased laser intensity (Fig. 2). All the cells in  
159 a branch, regardless whether they formed a “T” (Fig. 2) or (reverse) “Y” branch (not shown),  
160 showed recovery. A quantified analysis of recovery, shown for a specimen “T” branch in Fig. 2,  
161 in which the bleached out branch was defined as one region of interest (ROI), reveals that  
162 recovery is mediated by cells from both sides next to the branching point. The fluorescence  
163 intensity decreases in the adjacent cells over time. Accordingly our results demonstrate that  
164 trichomes of *M. laminosus* form a complex interconnected cell communication network. A newly  
165 formed branch remains connected to its main trichome.

166 The exchange of molecules between the cytoplasm of cells requires the presence of cell-to-cell  
167 connecting structures penetrating the peptidoglycan layer and the plasma membranes of both  
168 cells (e.g. Merino-Puerto *et al.*, 2011; Lehner *et al.*, 2013). The occurrence of such structures,  
169 which have been termed septosomes (or microplasmodesmata), has been well characterized in



170 *Anabaena* spp. by various methods, such as thin-section TEM (e.g. Wildon and Mercer, 1963),  
171 freeze-fracture EM (Giddings and Staehelin, 1978; Giddings and Staehelin, 1981) and electron  
172 tomography (Wilk *et al.*, 2011), but it has remained unclear whether septosomes exist in *M.*  
173 *laminosus*. A first indication of their presence in *M. laminosus* was given by Marcenko (1962),  
174 who could identify pores with an average diameter of 15 nm in the cross-walls of isolated cell  
175 wall sacculi. Our electron micrographs of thin sections through the septal regions of *M.*  
176 *laminosus* clearly show structures pervading the septa between vegetative cells (Fig. 3A) and  
177 between heterocysts and vegetative cells (Fig. 3B). Different methods of sample preparation for  
178 TEM can also be used to reveal insights into the composition of intercellular channels (Wilk *et*  
179 *al.*, 2011). Our results are in good agreement with the proposed proteinaceous nature of the  
180 septosomes found in *Anabaena* sp. PCC 7120 (Wilk *et al.*, 2011). While septosomes appear as  
181 positively stained structures in a  $\text{KMnO}_4$ -based preparation method (Fig. 3A), they are negatively  
182 stained in an  $\text{OsO}_4$ -based preparation (Fig. 3B).

183 Although the presence of pores penetrating the septum was shown earlier in *Stigonema*  
184 *hormoides*, *Fischerella muscicola*, and *F. ambigua*, which belong to cyanobacteria of Section V,  
185 it has been suggested that these pores do not pierce the underlying plasma membranes, and  
186 accordingly do not mediate a direct connection of the protoplasts (Thurston and Ingram, 1971;  
187 Butler and Allsopp, 1972). Our results from fluorescent dye exchange, however, show the  
188 connectivity of the cytoplasm throughout the entire filament network, which is likely achieved by  
189 structures resembling septosomes.

190

191 **Composition and localisation of SepJ in *M. laminosus* is similar to those found in**  
192 **cyanobacteria of Section IV**

193 Our ultrastructural studies of septa suggest that septosomes consist of proteins. In *Anabaena* sp.  
194 PCC 7120 a potential key player is SepJ. SepJ is not only necessary for filament integrity (Nayar  
195 *et al.*, 2007; Flores *et al.*, 2007; Merino-Puerto *et al.*, 2010) but also essential for intercellular  
196 exchange of molecules (Mullineaux *et al.*, 2008; Mariscal *et al.*, 2011). Although a *sepJ* deletion  
197 mutant still exhibits septosomes, the spacing between the two plasma membranes of the  
198 neighbouring vegetative cells is significantly reduced (Wilk *et al.*, 2011). We asked whether SepJ  
199 is also present in *M. laminosus*. Due to the lack of a genome sequence for this cyanobacterium,  
200 we designed primers based on DNA sequence similarity between the *sepJ* and the *hetR* sequences  
201 deposited in the GenBank® database (Benson *et al.*, 2011). *hetR* encodes a protein that is a  
202 master regulator of heterocyst differentiation in the Section IV cyanobacterium *Anabaena* sp.  
203 PCC 7120 (Buikema and Haselkorn, 1991), and is widely distributed among filamentous  
204 cyanobacteria, including non-heterocystous species (Zhang *et al.*, 2009). As *hetR* is usually  
205 located downstream of *sepJ* we selected a highly conserved region between six cyanobacterial  
206 strains of Section V within this gene, and defined it as primer rev\_mlam\_hetR (Fig. S2A). The  
207 design of primer fw\_mlam\_sepJ was based on an alignment of the *sepJ* sequences from four  
208 species, which are filamentous and heterocyst forming (Fig. S2B).

209 The PCR with both primers generated a DNA product that contained a sequence with a high  
210 similarity to *sepJ*. The corresponding amino acid sequence revealed that, similar to SepJ from  
211 Section IV cyanobacteria (Mariscal *et al.*, 2011), SepJ of *M. laminosus* consists of three domains,  
212 including a coiled-coil domain (CC), a highly repetitive linker region (L), and a permease domain  
213 (P). To find out whether there exists a correlation between the SepJ domain structure and its

214 distribution among cyanobacteria, we ran a BlastP search with the amino acid sequence of SepJ  
215 from *M. laminosus* as query against all cyanobacterial sequences available from the Integrated  
216 Microbial Genomes (IMG) database (Markowitz *et al.*, 2012), and against the recently published  
217 sequences by Dagan *et al.* (2013) (April 2013; Table S1). In our analysis we considered proteins  
218 which are comprised of either two or three domains ((CC+P) or (CC+L+P)) as SepJ-like proteins,  
219 whereas proteins showing only similarity to the permease domain were considered as DME-  
220 family permeases. Our analysis revealed that in 62 from 139 cyanobacterial species (45%) a  
221 SepJ-like protein is present, while only 28 cyanobacterial species (20%) possess DME-family  
222 permease, of which 16 (12%) can be found additionally in cyanobacteria possessing a SepJ-like  
223 protein. While all cyanobacteria of Sections IV and V (20 and 12 species respectively), and most  
224 species of Section III (32 from 34 species (94 %)) possess a SepJ-like protein, a SepJ variant is  
225 absent from unicellular species of Sections I and II, indicating the importance of SepJ for  
226 filamentous cyanobacteria. Furthermore, a closer look at the composition of the SepJ-like  
227 proteins in the different cyanobacterial sections reveals that filamentous species of Section III  
228 show mainly a two domain protein (CC+P) (23/32 species; 72%), and nearly all filamentous,  
229 heterocyst-forming (and branching) cyanobacteria of Sections IV and V exhibit a three-domain  
230 (CC+L+P) SepJ variant (20/20 species (100 %); and 11/12 species (92 %) respectively). We  
231 conclude that SepJ-like proteins containing a coiled-coil domain and a highly repetitive linker  
232 region of various lengths can be attributed to filamentous heterocystous cyanobacteria.

233 The amino acid sequence of SepJ from *M. laminosus* SAG 4.84 is almost identical to that of  
234 *Fischerella muscicola* PCC 7414 (Dagan *et al.*, 2013) despite the great spatial separation of their  
235 origins of isolation (Iceland and New Zealand) (Rippka *et al.*, 1979). Intercontinental dispersal  
236 e.g. by transpacific winds (Smith *et al.*, 2013) would explain the presence of “similar” strains of  
237 *M. laminosus* in such widely separated habitats. A phylogenetic analysis based on 16S rRNA

238 sequences (Fig. S3) strongly supports the close relationship between *F. muscicola* PCC 7414, *M.*  
239 *laminosus* SAG 4.84 and other strains from widely dispersed sites (Table S2). Although the  
240 amino acid sequence of SepJ from *M. laminosus* SAG 4.84 and *Fischerella* sp. PCC 7414 show a  
241 high similarity, it has to be pointed out that *sepJ* from *Fischerella* sp. PCC 7414 might bear a  
242 stop codon in the highly repetitive linker region.

243 In order to localise SepJ in *M. laminosus* we performed immunofluorescence labelling using the  
244 antibody against the coiled-coil domain of SepJ from *Anabaena* sp. PCC 7120 (Mariscal *et al.*,  
245 2011). The experiments show that SepJ is always located in the centre of intercellular septa of *M.*  
246 *laminosus* (Fig. 3C; Fig. S4; Fig. S5). There is also a dispersed background fluorescence signal in  
247 the cytoplasm, however this signal is also seen in the absence of the primary anti-SepJ antibody  
248 and therefore does not reflect SepJ localisation (Fig. S4). SepJ forms distinct spots not only in the  
249 main wide trichome, but also in the narrow branch (Fig. 3C). A newly-formed branching point  
250 shows three distinct regions of SepJ located to the adjacent cells (Fig. 3C). The positioning of  
251 SepJ likely takes place during the cell division, when the protein forms a ring at the division  
252 plane (Fig. S5). These findings are in good agreement with those in *Anabaena* sp. PCC 7120  
253 (Flores *et al.*, 2007) and support the importance of SepJ at the septal region of filamentous,  
254 heterocyst-forming cyanobacteria.

### 255 **Molecular exchange within the filament network is regulated, and depends on cell shape**

256 While branches are comprised of long, narrow, cylindrical cells, main trichomes consist of large,  
257 rounded-up cells (e.g. (Schwabe, 1960; Nierzwicki *et al.*, 1982). Although cells in branch and  
258 main trichomes show distinct differences in their cell shape, their ultrastructure is similar, varying  
259 mainly in the number of carboxysomes and peripherally located lipid bodies. Wide cells possess a  
260 higher number of these inclusions than narrow cells (Nierzwicki *et al.*, 1982; Nierzwicki-Bauer *et*

261 *al.*, 1984b), and it has been suggested that they might be functionally active rather than being in a  
262 resting state (Balkwill *et al.*, 1984). To gain further information about the possible function of  
263 these different morphotypes, we investigated the ability to exchange molecules by FRAP  
264 experiments with the fluorescent tracer 5-CFDA. A parameter to quantify the kinetics of dye  
265 exchange between cells is the “exchange coefficient” (E), which can be calculated as previously  
266 described (Mullineaux *et al.*, 2008). E has units of  $s^{-1}$  and relates the rate of molecular flux  
267 between adjacent cells to the difference in dye concentration between the cells. However, E is not  
268 the best parameter to use for making comparisons of the connectivity of morphotypes with  
269 significantly different cell volumes, because the concentration changes resulting from flux of  
270 molecules across the cell junction depend on cell volume as well as the flux across the junction.  
271 Therefore we introduce a new parameter, the “flux coefficient” F, defined as (E x cell volume),  
272 with units of  $\mu m^3 s^{-1}$ . F corrects for the influence of cell volume on E, to give a value that allows  
273 comparison of molecular exchange activity at junctions between different morphotypes.

274 To take the influence of the high degree of cell polymorphism in *M. laminosus* on the cell volume  
275 into account, we chose four different geometrical shapes, including cylinder, prolate spheroid,  
276 sphere, and oblate spheroid. While cylindrical cells were considered to represent cells in narrow  
277 trichomes, both spherical and spheroidal cells were considered to represent cells of wide  
278 trichomes. Our results indicate that cells in narrow trichomes exhibit significantly higher E and F  
279 values than cells in wide trichomes (Table 1), suggesting that not only the change in  
280 concentration of molecules but also the flux of molecules between cells depends on the trichome  
281 type. The mechanism which leads to the significant decrease in communication between cells  
282 during the process of maturation from a narrow to a wide trichome remains yet to be investigated.

283 A high degree of cell-cell communication might be essential to ensure a sufficient supply of  
284 nutrients and regulators within a fast-growing narrow trichome. To investigate this hypothesis,  
285 we considered further cell differentiation processes in *M. laminosus*, which are supposed to  
286 require cell-cell communication, including the formation of heterocysts and motile hormogonia.

287 Nitrogen limitation stimulates extensive heterocyst differentiation in *M. laminosus*. Almost any  
288 vegetative cell can differentiate into a heterocyst (Nierzwicki-Bauer *et al.*, 1984b; Stevens *et al.*,  
289 1985). Here we particularly focussed on the localisation of heterocysts in the region of branching.

290 Heterocysts were distinguished from vegetative cells by their diminished pigmentation and the  
291 presence of cyanophycin plugs at the cell poles. We observed that any cell in the branching  
292 region is capable of undergoing cell differentiation, resulting in the formation of heterocysts in  
293 the branching point of a “T”-branch and a (reverse) “Y”-branch (Fig. 4A-D). The position of the  
294 cyanophycin plugs in these cells is notable. Heterocysts at the origin of a branch show three  
295 cyanophycin plugs, while neighbouring heterocysts in the branching region of “T” and (reverse)  
296 “Y”-branches only possess two cyanophycin plugs (Fig. 4B,C). These microscopic observations  
297 support our previous FRAP results that *M. laminosus* forms a complex network of various  
298 trichome types, which exchange metabolites, including products of nitrogen and carbon fixation.  
299 The key function of the main trichomes might be to provide the basis for growth of the organism  
300 under favourable environmental conditions.

301 Earlier observations by Nierzwicki-Bauer *et al.* (1984a) that *M. laminosus* forms multiple  
302 contiguous heterocysts in the main trichomes under nitrogen deprivation support this hypothesis.

303 Although we rarely observed the formation of multiple contiguous heterocysts in the main  
304 trichome of *M. laminosus* SAG 4.84, we regularly found double heterocysts in the branches (Fig.  
305 4E). It is possible that the different heterocyst localisation is caused either by the altered growth

306 conditions or the diversity of *M. laminosus* strains in general, since a strain of *M. laminosus* Cohn  
307 has been described which lacks the ability to form heterocysts (Melick *et al.*, 1991). The  
308 formation of double heterocysts is again interesting with regard to the position of cyanophycin  
309 plugs. Each heterocyst shows two cyanophycin plugs, resulting in a double cyanophycin plug  
310 between both heterocysts (Fig. 4E). Until now the role of cyanophycin (multi-L-arginyl-poly-L-  
311 aspartic acid) has remained unclear, though a role as a dynamic nitrogen reserve is likely due to  
312 its high nitrogen content of approximately 26% of its mass (Lockau and Ziegler, 2006).

313 To characterise the heterocyst-heterocyst connection further we used the fluorescent dye FM1-  
314 43FX (Schneider *et al.*, 2007). Our results clearly show that both heterocysts are connected via  
315 two neck regions (Fig. S6). Overall, heterocysts of *M. laminosus* seem to be much more strongly  
316 connected to their neighbouring cells than in *Anabaena* spp. since we never observed any single  
317 heterocysts or short filaments with terminal heterocysts.

318 Another important stage in the life cycle of *M. laminosus* is the formation of hormogonia, motile  
319 filaments which glide slowly away from the parental filament, before finally differentiating into a  
320 sedentary wide trichome and forming a new colony (Hernandez-Muniz and Stevens, 1987).  
321 Hormogonia show a high variability in surface velocity, which differs not only between  
322 hormogonia but also for the same hormogonium over time, and a high variability in the directions  
323 they move (Hernandez-Muniz and Stevens, 1987). Their ability to reverse the direction of gliding  
324 (Hernandez-Muniz and Stevens, 1987) suggests a high degree of cell-cell communication. In  
325 order to determine the exchange and flux coefficient for hormogonia we chose to measure the cell  
326 dimensions of a moving hormogonium, and correlate them to the tracer exchange data  
327 represented earlier. This ensures that also hormogonia are considered which were not moving  
328 during the FRAP experiments. As hormogonia are formed by cell division without biomass

329 increase, they can be distinguished from other filament types by their distinctly smaller cell size  
330 (Campbell and Meeks, 1989). Accordingly, we defined hormogonia of *M. laminosus* by cell  
331 diameter, cell length, and the diameter to length ratio, resulting in a group of cells characterised  
332 by an average cell diameter of  $2.76 \pm 0.31 \mu\text{m}$ , an average cell length of  $3.61 \pm 0.88 \mu\text{m}$ , and a  
333 diameter to length ratio of  $0.80 \pm 0.19$  (n=80). While the mean exchange coefficient E is similar  
334 to that found between cells in narrow trichomes ( $E = 0.159 \pm 0.072 \text{ s}^{-1}$ ) and meets the expectation  
335 that cellular communication is fast in hormogonia, the flux coefficient F is significantly lower,  
336 showing a value similar to that found in wide trichomes ( $F = 3.60 \pm 2.47 \mu\text{m}^3 \text{ s}^{-1}$ ) (Table 1).  
337 Therefore communication between cells in hormogonia is rapid in the sense that intercellular  
338 diffusion of molecules is fast enough to lead to rapid changes in the cytoplasmic concentration of  
339 putative signalling molecules. However, as compared to cells in the parental filament, this rapid  
340 communication is achieved by reducing the cell volume rather than by accelerating the flux of  
341 molecules across the cell junctions. Therefore signal transduction to coordinate movement (and  
342 possibly other aspects of the biology) of hormogonia is probably accelerated by the reduction of  
343 the cell volume rather than by increased flux of signalling molecules across the cell junctions.

#### 344 **Barriers to cell-cell communication are formed early in the life cycle of *M. laminosus***

345 The release of a hormogonium from its parental trichome is mediated by the formation of  
346 releasing, dead cells, called necridia, which are possibly best studied in *Oscillatoria/Microcoleus*  
347 spp. (Kohl, 1903; Lamont, 1969; Brown *et al.*, 2010). Beside heterocysts (Meeks *et al.*, 2002),  
348 necridia are one of the few known developmental “dead ends” among prokaryotes, and can be  
349 seen as a basic form of programmed cell death (apoptosis). Since a necridium can be found early  
350 after the branching event in the growing narrow trichome (Fig. 5A-C), we investigated whether  
351 exchange of molecules is still possible between the branch and the main trichome. After loading



352 the fluorescent tracer 5-CFDA into the cytoplasm, we bleached out the fluorescence of the part of  
353 the branch which was separated by the necridium and followed its change in fluorescence  
354 intensity (Fig. 5A). We did not observe any recovery of the bleached region within 24 s (Fig. 5A)  
355 indicating that a necridium inhibits cell-cell communication completely. Accordingly, the fate of  
356 a trichome is determined early after branch formation; molecular exchange not being possible  
357 once a necridium is formed.

358 To get an impression of the complexity of this event and its importance for the filamentous  
359 network, we investigated the position of necridium formation. Necridia can be easily detected by  
360 enhanced red fluorescence in the region of formation, possibly as a result of degradation of the  
361 photosynthetic apparatus (Figs. 5B-D and 6A). Necridia also show brighter staining with the  
362 membrane dye FM1-43FX (Fig 5B-D), probably because leakiness of the cytoplasmic membrane  
363 allows the dye to penetrate to the interior of the cell. We observed that necridia are not only  
364 located in the branching point, as reported in an earlier study (Balkwill *et al.*, 1984), but also in  
365 various other positions within narrow trichomes, such as the beginning of the recently formed  
366 branch (Fig. 5C), indicating that almost any cell within a filament can differentiate into a  
367 necridium. Even within the same filament several necridia can be found, contiguous or separated  
368 only by a single cell (Fig. 5D), suggesting that necridia formation in *M. laminosus* seems to  
369 follow no regular pattern of spacing and distribution.

370  
371 The final release of the trichome is a complex mechanism of remodelling the septal region on  
372 both sides of the necridium. To avoid cell death of the entire cellular network by efflux of  
373 molecules, the membranes of the neighbouring cells have to stay intact, and the channels/pores  
374 have to be closed. Electron micrographs confirm that the plasma membrane and outer membrane

375 are sealed at the terminal cell (Fig. 6B). Although we observed that necridia usually consist only  
376 of a single cell, they can be formed by two cells (Fig. 5B, D). A possible mechanism to prevent  
377 efflux of molecules in other cyanobacteria, e.g. *Symploca muscorum* and *M. vaginatus* might be  
378 by the synthesis of an additional cell wall layer at the new terminus (“calyptra”; Pankratz and  
379 Bowen, 1963; Lamont, 1969). It remains yet to be investigated whether this structure also exists  
380 in *M. laminosus*.

381 Filament breakage, however, is only possible by the disintegration of the membranes of the  
382 necridium. To investigate this process we used the cytoplasmic membrane stain FM1-43FX (Fig.  
383 5B,C,D) and the DNA stain Hoechst 33258 (Fig. 6A). The fluorescence micrographs indicate that  
384 during necridium formation the cytoplasmic membrane of the necridium deteriorates mainly from  
385 one terminus of the cell (Fig. 5B,C,D), leaving an “open” and empty (DNA-free) cell attached to  
386 the released filament (Fig. 6), while only a small part of membranes remains at the terminus of  
387 the parental filament.

### 388 Concluding remarks

389 Our results demonstrate that *M. laminosus* represents a complex cellular network, in which the  
390 main trichome and branches communicate via intercellular connections which resemble  
391 septosomes. We observed that exchange between cells within a culture is regulated, depending on  
392 cell morphology. Young, narrow trichomes exhibited rapid exchange rates among cells, while  
393 old, wide trichomes showed reduced rates. Accordingly, wide trichomes might not only provide a  
394 platform for the outgrowth of branches, but they might also support the growth of branches by  
395 supplying metabolites in the presence and absence of a combined nitrogen source. Under nitrogen  
396 deprivation heterocysts can be found frequently in the branching region, sometimes even in the  
397 branching start, forming a heterocyst with three cyanophycin plugs. The integrity of the filament

398 network is only interrupted by the formation of necridia, which inhibit further molecular  
399 exchange, and hence determine the fate of a developing branch likely to become a hormogonium,  
400 soon after the branching event. Interestingly, signal transduction to coordinate movement of the  
401 released hormogonia might be accelerated by the reduction in cell volume.

402 Cell differentiation seems to be generally less regulated than in Section IV cyanobacteria; the  
403 formation of heterocysts (Nierzwicki-Bauer *et al.*, 1984a; Nierzwicki-Bauer *et al.*, 1984b;  
404 Stevens *et al.*, 1985) and necridia (this study) seem to follow no regular spacing and distribution  
405 pattern. Our analyses of the different types of branches also suggest a degree of randomness in  
406 cell development. We hypothesise that “T” and “Y” branches are basically equivalent: the  
407 different forms simply result from loose control of the positioning of the cell elongation  
408 machinery.

409 As a possible component of the cell-cell connecting structures we identified SepJ. The protein  
410 consists of the typical three domain architecture found in other filamentous, heterocyst-forming  
411 cyanobacteria (Section IV), and immunofluorescence labelling revealed its localisation at the  
412 septa. A cell in the branching point exhibits three SepJ spots, suggesting that although *M.*  
413 *laminosus* shows branching, the septa are similar to those described in *Anabaena* sp. PCC 7120.

414 Earlier studies had suggested that rounded cells in wide trichomes are completely separated by  
415 their surrounding sheath (Thurston and Ingram, 1971; Martin and Wyatt, 1974; Nierzwicki *et al.*,  
416 1982) which would imply a lack of communication between these cells. According to our  
417 ultrastructural and FRAP analyses this is however not the case. *M. laminosus* shows intercellular  
418 communication and highly-structured cell junctions between cells of various shapes, forming a  
419 complex network of cell communication. The hypothesis that cyanobacteria of Section V  
420 represent a primitive and basic form linking coccoid and filamentous forms (Martin and Wyatt,

421 1974), is not supported by our study. Our results from cell division and intercellular  
422 communication experiments indicate that Section V cyanobacteria are similar to cyanobacteria of  
423 Section IV. Section IV and V cyanobacteria show the highest degree of morphological  
424 complexity and diversity within the phylum.

425

Accepted Article

## 426 Experimental Procedures

### 427 **Organism, medium, and growth.**

428 *Mastigocladus laminosus* SAG 4.84 was originally isolated by G. H. Schwabe from a thermal  
429 spring of Reyhjaness/Isafjord, Iceland in 1967. The cyanobacterium was grown in liquid  
430 Castenholz D medium (Castenholz, 1988) at 40°C, under constant white light at approximately  
431 20  $\mu\text{E m}^{-2} \text{ s}^{-1}$ . To provide constant agitation cultures were bubbled with sterile air or shaken (100  
432 rpm). For studies of intercellular communication between branch and main trichome, a resting  
433 culture was used to inoculate Castenholz D medium. After 24 h of growth cultures were loaded  
434 with 5-CFDA, and its transfer demonstrated by FRAP. Heterocyst differentiation was induced by  
435 growth for up to 96 h in Castenholz ND medium (Castenholz, 1988), which lacks combined  
436 nitrogen, under the above described conditions.

### 437 **Labelling with fluorescent dyes.**

438 For molecular exchange experiments, cells were labelled with the fluorescent tracers 5-  
439 carboxyfluorescein diacetate (5-CFDA; Molecular Probes) or calcein (Molecular Probes). 1 ml of  
440 *M. laminosus* culture was harvested by centrifugation (3000xg, 2 min.), washed twice and  
441 resuspended in 1 ml fresh growth medium, and mixed with 12  $\mu\text{l}$  of a 1  $\text{mg ml}^{-1}$  5-CFDA or  
442 calcein, acetoxymethyl ester solution in dimethylsulphoxide. The suspension with 5-CFDA was  
443 incubated for 30 min at 40°C in the dark with shaking in an orbital incubator at 80 rpm, and the  
444 suspension with calcein for 90 min under the same conditions. To remove the fluorescent dyes,  
445 the cells were washed three times in growth medium, and incubated for another 30 min in 1 ml of  
446 medium at 40°C in the dark under gentle shaking (80 rpm). After a final washing step, cells were  
447 spotted onto a Castenholz D 1.5 % (w/v) agar plate, and excess solution was removed. To

448 maintain the growth conditions throughout the experiment media and plates were preheated to  
449 40°C.

450 Two additional fluorescent dyes, FM1-43FX and Hoechst 33258, were used to visualise specific  
451 cellular components. FM1-43FX stains the outer and cytoplasmic membranes of cyanobacteria  
452 (Schneider *et al.*, 2007), while Hoechst 33258 interacts with DNA. For labelling, we washed cells  
453 once in fresh growth medium, and added 1 µl Hoechst 33258 (1 mg ml<sup>-1</sup>; Bisbenzimidazole H33258;  
454 AppliChem) and/or 2.5 µl FM1-43FX (0.1 mg ml<sup>-1</sup>; Molecular Probes) to 0.5 ml of culture. The  
455 suspension was incubated for 10 min at room temperature and washed twice with growth medium  
456 prior mounting on 1.5 % (w/v) agar with Castenholz D or ND medium. Surplus medium was  
457 removed.

#### 458 **Confocal microscopy and Fluorescence Recovery after Photobleaching (FRAP).**

459 For confocal microscopy, small blocks of agar were placed in a custom-built temperature-  
460 controlled sample holder covered with a glass cover slip. Cells were visualised with the Leica  
461 laser-scanning confocal microscope SP5 using a x63 oil-immersion objective (Leica HCX PL  
462 APO lambda blue 63.0x1.40 OIL UV), and an excitation wave length of 488 nm for 5-CFDA,  
463 calcein and FM1-43FX, and 355 nm for the Hoechst 33258-DNA complex. Chlorophyll *a*  
464 fluorescence (autofluorescence) and dye fluorescence were imaged simultaneously, using  
465 different emission detection ranges (455-495 nm for Hoechst 33258, 500-527 nm for 5-CFDA  
466 and calcein, 570-595 nm for FM1-43X, and 670-720 nm for the autofluorescence). For imaging,  
467 we used a 95 µm confocal pinhole, giving a resolution of 0.8 µm in the Z-direction (full width at  
468 half-maximum of the point-spread function), whereas we opened the pinhole maximal for FRAP  
469 measurements (600 µm, an optical section thickness of 4.2 µm respectively). After taking an

470 initial image (pre-bleach), the region of interest (ROI) was bleached by increasing the laser  
471 intensity and zooming into the ROI, and recovery was recorded. Images were taken typically in  
472 0.534 s intervals. FRAP data were analysed as described in (Mullineaux *et al.*, 2008) to estimate  
473 the exchange coefficient E, using Image Pro Plus 6.3 (Media Cybernetics Inc.) and SigmaPlot  
474 10.0 (Systat Software Inc.).

#### 475 **Electron Microscopy.**

476 Cultures were harvested by centrifugation (3000xg; 2 min) and fixed for 2 h at room temperature  
477 with 4% (w/v) glutaraldehyde in 100 mM phosphate buffer pH 7.3. To remove the fixative, cells  
478 were washed three times with 100 mM phosphate buffer. After embedding in 2% (w/v) low-  
479 gelling temperature agarose, samples were cut in one- to two-millimetre cubic blocks, and post-  
480 fixed with 2% (w/v) potassium permanganate dissolved in distilled water over night at 4°C.  
481 Samples were washed with distilled water until the supernatant remained clear, and dehydrated  
482 through a graded ethanol series (1x15 min 30%, 1x15 min 50%, 1x15 min 70%, 1x15 min 90%  
483 and 3x20 min 100%). Two washes for 5min with propylene oxide were performed prior  
484 infiltration with Araldite for 1 h and with fresh Araldite over night. Polymerisation was achieved  
485 by incubation at 60-65°C for 48 h. Alternatively, cells were fixed for 2h at room temperature in  
486 100 mM phosphate buffer pH 7.0 containing 3% (w/v) glutaraldehyde, 1% (w/v) formaldehyde  
487 and 0.5% (w/v) tannic acid, washed with phosphate buffer, and incubated in 2% (w/v) OsO<sub>4</sub> in  
488 phosphate buffer over night. Dehydration was performed using a graded acetone series as  
489 described for ethanol prior to embedding in Araldite. Thin sections were cut with a glass knife at  
490 a Reichert Ultracut E microtome and collected on uncoated, 300 mesh copper grids. High  
491 contrast was obtained by poststaining with saturated aqueous uranyl acetate and lead citrate

492 (Reynolds, 1963) for 4 min each. The grids were examined in a JOEL JEM-1230 transmission  
493 electron microscope at an accelerating potential of 80kV.

494

#### 495 **DNA isolation, gene amplification, and sequencing.**

496 Genomic DNA from *M. laminosus* was extracted using the protocol of Morin *et al.* (2010) with a  
497 cell homogenization step prior cell lysis. The cells were harvested by centrifugation (3,000xg, 5  
498 min) and resuspended in fresh growth medium. Homogenization of the culture was achieved by  
499 multiple passages through a 0.8 mm needle with the help of a syringe. The cells were collected by  
500 centrifugation (3000xg, 5 min), and genomic DNA was isolated as previously described (Morin  
501 *et al.*, 2010)

502 To identify *sepJ* in *M. laminosus* oligonucleotide primers were designed as follows: Since there  
503 were no *sepJ* sequences known from *M. laminosus* and other species of Section V, we assumed a  
504 similarity in its sequence and localisation to other filamentous, heterocyst-forming cyanobacteria.  
505 *sepJ* nucleotide sequences from *Anabaena* sp. PCC 7120, *Anabaena variabilis* ATCC 29413,  
506 '*Nostoc azollae*' 0708 and *Nostoc punctiforme* PCC 73102 were obtained from the NCBI  
507 GenBank and aligned with Clustal W 2.1 (Larkin *et al.*, 2007). The first 20 nucleotides built  
508 primer fw\_mlam\_sepJ (5'-atggggcgatttgagaagcg-3') (Fig. S2B). The reverse primer was designed  
509 on the assumption that *hetR* is located downstream of *sepJ*. Available partial *hetR* sequences from  
510 cyanobacteria of Section V (*Fischerella* spp. and *Chlorogloeopsis* spp.) were used for a Clustal  
511 W 2.1 alignment, and resulted in primer rev\_mlam\_hetR (5'-gttgcggctgcatctaaaa-3') (Fig. S2A).

512 The optimal annealing temperature for *sepJ* amplification was determined by using a gradient  
513 PCR with the Promega PCR Master Mix. PCR products were resolved by electrophoresis in a 1%



514 (w/v) agarose gel. The final amplification was performed with the Roche Expand High Fidelity  
515 PCR System using the following conditions for a 50µl reaction: 94°C for 2 min, 15x cycle 1  
516 (94°C for 45 sec; 48.9°C for 45 sec; 72°C for 4 min), 15x cycle 2 (94°C for 45 sec; 59°C for 45  
517 sec; 72°C for 4 min) and 1x cycle 3 (94°C for 45 sec; 57°C for 45 sec; 72°C for 10 min).

518 The amplified product was checked on a 1% (w/v) agarose gel, and purified with the QIAquick  
519 PCR purification kit (QIAGEN) for sequencing.

#### 520 **Nucleotide sequence accession number.**

521 The identified *sepJ* sequence has been deposited in the GenBank database under the accession  
522 number KF729033.

#### 523 **Sequence analysis.**

524 The *sepJ* DNA sequence was translated into the corresponding amino acid sequence using the  
525 ExPASy translate tool (<http://web.expasy.org/translate/>). A BlastP search was performed in order  
526 to identify orthologous sequences (Altschul *et al.*, 1997). Further sequence analyses were  
527 performed using the TMHMM server 2.0 (<http://www.cbs.dtu.dk/services/TMHMM/>) in order to  
528 predict the localisation of transmembrane helices, TRUST (Szklarczyk and Heringa, 2004) for  
529 the detection of internal repeats, and Coils/PCoils (<http://toolkit.tuebingen.mpg.de/pcoils>) for the  
530 identification of potential coiled-coiled regions in SepJ.

#### 531 **Immunofluorescence labelling and sample examination.**

532 Cells were harvested by centrifugation (3000xg; 2 min) and resuspended in fresh growth medium.  
533 Cultures were transferred onto 0.2 µm Nucleopore membranes, which were subsequently placed  
534 onto poly-L-lysine coated slides. For fixation the slides were incubated in 50-ml plastic Falcon

535 tubes containing 70% (v/v) chilled (-20°C) ethanol for 30 min at -20°C. After 3 washing steps for  
536 2 min with phosphate-buffered saline (PBS: 137 mM NaCl, 2.7 mM KCl, 10 mM phosphate  
537 buffer) with 0.1 % (v/v) Tween 20 (PBST), the samples were immersed in 3% (w/v) milk  
538 powder, diluted in PBST, and incubated for 15 min at room temperature. Afterwards, the slides  
539 were directly incubated with the primary antibody, rabbit anti-*Anabaena* sp. PCC 7120 SepJ  
540 (Mariscal *et al.*, 2011), diluted 1:250 in PBST, and stored for 3 h at 30°C in a moisture chamber.  
541 After incubation, the samples were washed three times in PBST for 2 min, and then incubated  
542 with the secondary antibody for 45 min at 30°C. The secondary antibody was an anti-rabbit  
543 immunoglobulin G conjugated with Alexa Fluor 488 (Invitrogen) diluted 1:500 in PBST. After  
544 final washing steps with PBST (3x 2 min), the slides were mounted with a cover slip using  
545 FluorSave™ Reagent (Calbiochem), and sealed with nail varnish.

546 Immunolabelled cells were examined with a Leica DM6000B fluorescence microscope, using an  
547 x63 oil-immersion objective and an ORCA-ER camera (Hamamatsu). Alexa Fluor 488  
548 fluorescence was monitored using a fluorescein isothiocyanate (FITC) L5 filter (excitation, band-  
549 pass [BP] 480/40 filter; emission, BP 527/30 filter), and autofluorescence was monitored using a  
550 Texas Red TX2 filter (excitation, BP 560/40; emission, BP 645/75). Images were convolved with  
551 the Leica Application Suite Advanced Fluorescence software.

## 552 Acknowledgements

553 We are especially grateful to Karina Stucken for advice on identifying *sepJ*. Furthermore, we  
554 thank Graham McPhail and Petra Ungerer for their support in electron microscopy, and Igor  
555 Brown, Jiří Komárek, and Damir Viličić for providing literature on various topics.

556 This work was supported by a college studentship of Queen Mary University of London, and the  
557 College Central Research Fund. Work in Seville was supported by grant no. BFU2011-22762  
558 from Plan Nacional de Investigación, Spain, co-financed by FEDER.

559 The authors declare no conflict of interest.

560

Accepted Article

561

## 562 References

- 563 Altschul, S.F., Madden, T.L., Schäffer, A.A., Zhang, J., Zhang, Z., Miller, W., and Lipman, D.J. (1997)  
564 Gapped BLAST and PSI-BLAST: a new generation of protein database search programs. *Nucl Acids Res*  
565 **25**: 3389–3402.
- 566 Anagnostidis, K., and Komárek, J. (1990) Modern approach to the classification system of Cyanophytes.  
567 5-Stigonematales. *Arch Hydrobiol Suppl Algal Stud* **59**: 1–73.
- 568 Balkwill, D.L., Nierzwicki-Bauer, S.A., and Stevens, S.E.J. (1984) Modes of cell division and branch  
569 formation in the morphogenesis of the cyanobacterium *Mastigocladus laminosus*. *J Gen Microbiol* **130**:  
570 2079–2088.
- 571 Bekker, A., Holland, H.D., Wang, P.-L., Rumble, D., Stein, H.J., Hannah, J.L., *et al.* (2004) Dating the  
572 rise of atmospheric oxygen. *Nature* **427**: 117–20.
- 573 Benson, D.A., Karsch-Mizrachi, I., Lipman, D.J., Ostell, J., and Sayers, E.W. (2011) GenBank. *Nucl*  
574 *Acids Res* **39**: D32–D37.
- 575 Brown, I.I., Bryant, D.A., Casamatta, D., Thomas-Keprta, K.L., Sarkisova, S.A., Shen, G., *et al.* (2010)  
576 Polyphasic characterization of a thermotolerant siderophilic filamentous cyanobacterium that produces  
577 intracellular iron deposits. *Appl Env Microbiol* **76**: 6664–6672.
- 578 Buikema, W.J., and Haselkorn, R. (1991) Characterization of a gene controlling heterocyst differentiation  
579 in the cyanobacterium *Anabaena* 7120. *Genes Dev* **5**: 321–330.
- 580 Butler, R.D., and Allsopp, A. (1972) Ultrastructural investigations in the Stigonemataceae (Cyanophyta).  
581 *Arch Microbiol* **82**: 283–299.
- 582 Campbell, E.L., and Meeks, J.C. (1989) Characteristics of hormogonia formation by symbiotic *Nostoc*  
583 spp. in response to the presence of *Anthoceros punctatus* or its extracellular products. *Appl Env Microbiol*  
584 **55**: 125–131.
- 585 Castenholz, R.W. (1976) The effect of sulfide on the bluegreen algae of hot springs. New Zealand and  
586 Iceland. *J Phycol* **12**: 54–68.
- 587 Castenholz, R.W. (1988) Culturing methods for cyanobacteria. *Methods Enzymol* **167**: 68–93.
- 588 Cohn, F. (1862) Über die Algen des Karlsbader Sprudels, mit Rücksicht auf die Bildung des  
589 Sprudelsinesters. *Abhandlungen der schlesischen Gesellschaft für vaterländische Kultur* **5**: 37–55.
- 590 Croft, W.N., and George, E.A. (1959) Blue-green algae from the Middle Devonian of Rhynie,  
591 Aberdeenshire. *Bull Br Museum Nat Hist Geol* 341–353.

- 592 Dagan, T., Roettger, M., Stucken, K., Landan, G., Koch, R., Major, P., *et al.* (2013) Genomes of  
593 stigonematalean cyanobacteria (Subsection V) and the evolution of oxygenic photosynthesis from  
594 prokaryotes to plastids. *Genome Biol Evol* **5**: 31–44.
- 595 Desikachary, T. V (1959) *Cyanophyta*. Indian Council of Agricultural Research, New Delhi, India.
- 596 Finsinger, K., Scholz, I., Serrano, A., Morales, S., Uribe-lorio, L., Mora, M., *et al.* (2008) Characterization  
597 of true-branching cyanobacteria from geothermal sites and hot springs of Costa Rica. *Env Microbiol* **10**:  
598 460–473.
- 599 Flores, E., and Herrero, A. (2010) Compartmentalized function through cell differentiation in filamentous  
600 cyanobacteria. *Nat Rev Microbiol* **8**: 39–50.
- 601 Flores, E., Pernil, R., Muro-Pastor, A.M., Mariscal, V., Maldener, I., Lechno-Yossef, S., *et al.* (2007)  
602 Septum-localized protein required for filament integrity and diazotrophy in the heterocyst-forming  
603 cyanobacterium *Anabaena* sp. strain PCC 7120. *J Bacteriol* **189**: 3884–3890.
- 604 Fogg, G.E., Stewart, W.D.P., Fay, P., and Walsby, A.E. (1973) *The Blue-Green Algae*. Academic Press,  
605 London and New York.
- 606 Geitler, L. (1960) *Schizophyzeen*. Gebrüder Borntraeger, Berlin-Nikolassee, Germany.
- 607 Giddings, T.H.J., and Staehelin, L.A. (1978) Plasma membrane architecture of *Anabaena cylindrica*:  
608 occurrence of microplasmodesmata and changes associated with heterocyst development and the cell cycle.  
609 *Cytobiologie* **16**: 235–249.
- 610 Giddings, T.H.J., and Staehelin, L.A. (1981) Observation of microplasmodesmata in both heterocyst-  
611 forming and non-heterocyst forming filamentous cyanobacteria by freeze-fracture electron microscopy.  
612 *Arch Microbiol* **129**: 295–298.
- 613 Golubić, S., Hernandez-Marine, M., and Hoffmann, L. (1996) Developmental aspects of branching in  
614 filamentous Cyanophyta/Cyanobacteria. *Arch Hydrobiol Suppl Algal Stud* **83**: 303–329.
- 615 Hernandez-Muniz, W., and Stevens, S.E.J. (1987) Characterization of the motile hormogonia of  
616 *Mastigocladus laminosus*. *J Bacteriol* **169**: 218–223.
- 617 Kohl, F.G. (1903) *Über die Organisation und Physiologic der Cyanophyeeenzelle und die mitotische*  
618 *Teilung ihres Kernes*. Gustav Fischer, Jena, Germany.
- 619 Komárek, J., and Anagnostidis, K. (1989) Modern approach to the classification system of cyanophytes.  
620 4-Nostocales. *Algal Stud* **56**: 247–345.
- 621 Komárek, J., Kling, H., and Komárková, J. (2003) Filamentous cyanobacteria. In *Freshwater Algae of*  
622 *North America*. Wehr, J.D., and Sheath, R.G. (eds). Elsevier Inc., pp. 117–196.
- 623 Konhauser, K.O., Lalonde, S. V, Planavsky, N.J., Pecoits, E., Lyons, T.W., Mojzsis, S.J., *et al.* (2011)  
624 Aerobic bacterial pyrite oxidation and acid rock drainage during the Great Oxidation Event. *Nature* **478**:  
625 369–373.

- 626 Lamont, H.C. (1969) Sacrificial cell death and trichome breakage in an Oscillatoriacean blue-green alga:  
627 the role of murein. *Arch Microbiol* **69**: 237–259.
- 628 Larkin, M.A., Blackshields, G., Brown, N.P., Chenna, R., McGettigan, P. a, McWilliam, H., *et al.* (2007)  
629 Clustal W and Clustal X version 2.0. *Bioinformatics* **23**: 2947–2948.
- 630 Lehner, J., Berendt, S., Dörsam, B., Pérez, R., Forchhammer, K., and Maldener, I. (2013) Prokaryotic  
631 multicellularity: a nanopore array for bacterial cell communication. *FASEB J* **27**: 1–8.
- 632 Lockau, W., and Ziegler, K. (2006) Cyanophycin Inclusions: Biosynthesis and Applications. In *Microbial*  
633 *Bionanotechnology: Biological Self-Assembly Systems and Biopolymer-Based Nanostructures*. Rehm, B.  
634 (ed.). Horizon Scientific Press, pp. 79–106.
- 635 Mackenzie, R., Pedrós-Alió, C., and Díez, B. (2013) Bacterial composition of microbial mats in hot  
636 springs in Northern Patagonia: variations with seasons and temperature. *Extremophiles* **17**: 123–36.
- 637 Marcenko, E. (1962) Licht- und elektronenmikroskopische Untersuchungen an der Thermalalge  
638 *Mastigocladus laminosus* Cohn. *Acta Bot Coratica* **20/21**: 47–74.
- 639 Mariscal, V., Herrero, A., Nenninger, A., Mullineaux, C.W., and Flores, E. (2011) Functional dissection  
640 of the three-domain SepJ protein joining the cells in cyanobacterial trichomes. *Mol Microbiol* **79**: 1077–  
641 1088.
- 642 Markowitz, V.M., Chen, I.-M.A., Palaniappan, K., Chu, K., Szeto, E., Grechkin, Y., *et al.* (2012) IMG:  
643 the Integrated Microbial Genomes database and comparative analysis system. *Nucl Acids Res* **40**: D115–  
644 D122.
- 645 Martin, T.C., and Wyatt, J.T. (1974) Comparative physiology and morphology of six strains of  
646 Stigonematacean blue-green algae. *J Phycol* **10**: 57–65.
- 647 Meeks, J.C., Campbell, E.L., Summers, M.L., and Wong, F.C. (2002) Cellular differentiation in the  
648 cyanobacterium *Nostoc punctiforme*. *Arch Microbiol* **178**: 395–403.
- 649 Melick, D.R., Broady, P.A., and Rowan, K.S. (1991) Morphological and physiological characteristics of a  
650 non-heterocystous strain of the cyanobacterium *Mastigocladus laminosus* Cohn from fumarolic soil on Mt  
651 Erebus , Antarctica. *Polar Biol* 81– 89.
- 652 Merino-Puerto, V., Mariscal, V., Mullineaux, C.W., Herrero, A., and Flores, E. (2010) Fra proteins  
653 influencing filament integrity, diazotrophy and localization of septal protein SepJ in the heterocyst-  
654 forming cyanobacterium *Anabaena* sp. *Mol Microbiol* **75**: 1159–70.
- 655 Merino-Puerto, V., Schwarz, H., Maldener, I., Mariscal, V., Mullineaux, C.W., Herrero, A., and Flores, E.  
656 (2011) FraC/FraD-dependent intercellular molecular exchange in the filaments of a heterocyst-forming  
657 cyanobacterium, *Anabaena* sp. *Mol Microbiol* **82**: 87–98.
- 658 Miller, S.R., Purugganan, M.D., and Curtis, S.E. (2006) Molecular Population Genetics and Phenotypic  
659 Diversification of Two Populations of the Thermophilic Cyanobacterium *Mastigocladus laminosus*. *Appl*  
660 *Env Microbiol* **72**: 2793–2800.

- 661 Morin, N., Vallaey, T., Hendrickx, L., Natalie, L., and Wilmotte, A. (2010) An efficient DNA isolation  
662 protocol for filamentous cyanobacteria of the genus *Arthrospira*. *J Microbiol Methods* **80**: 148–154.
- 663 Mullineaux, C.W., Mariscal, V., Nenninger, A., Khanum, H., Herrero, A., Flores, E., and Adams, D.G.  
664 (2008) Mechanism of intercellular molecular exchange in heterocyst-forming cyanobacteria. *EMBO J* **27**:  
665 1299–1308.
- 666 Nayar, A.S., Yamaura, H., Rajagopalan, R., Risser, D.D., and Callahan, S.M. (2007) FraG is necessary for  
667 filament integrity and heterocyst maturation in the cyanobacterium *Anabaena* sp. strain PCC 7120.  
668 *Microbiology* **153**: 601–607.
- 669 Nierzwicki, S.A., Maratea, D., Balkwill, D.L., Hardie, L.P., Mehta, V.B., and Stevens, S.E.J. (1982)  
670 Ultrastructure of the cyanobacterium, *Mastigocladus laminosus*. *Arch Microbiol* **133**: 11 – 19.
- 671 Nierzwicki-Bauer, S.A., Balkwill, D.L., and Stevens, S.E.J. (1984a) Heterocyst differentiation in the  
672 cyanobacterium *Mastigocladus laminosus*. *J Bacteriol* **157**: 514–525.
- 673 Nierzwicki-Bauer, S.A., Balkwill, D.L., and Stevens, S.E.J. (1984b) Morphology and ultrastructure of the  
674 cyanobacterium *Mastigocladus laminosus* growing under nitrogen-fixing conditions. *Arch Microbiol* **137**:  
675 97–103.
- 676 Pankratz, H.S., and Bowen, C.C. (1963) Cytology of Blue-Green Algae. I. The Cells of *Symploca*  
677 *muscorum*. *Amer J Bot* **50**: 387–399.
- 678 Reynolds, E.S. (1963) The use of lead citrate at high pH as an electron-opaque stain in electron  
679 microscopy. *J Cell Biol* **17**: 208–212.
- 680 Rippka, R., Deruelles, J., Waterbury, J.B., Herdman, M., and Stanier, R.Y. (1979) Generic assignments,  
681 strain histories and properties of pure cultures of cyanobacteria. *J Gen Microbiol* **111**: 1–61.
- 682 Robinson, W.B., Meador, A.E., Stevens, S.E.J., and Ospeck, M. (2007) Measuring the force production of  
683 the hormogonia of *Mastigocladus laminosus*. *Biophys J* **93**: 699–703.
- 684 Schirrmeyer, B.E., Anisimova, M., Antonelli, A., and Bagheri, H.C. (2011) Taxa required for improved  
685 phylogenomic approaches. *BMC Evol Biol* **4**: 424–427.
- 686 Schneider, D., Fuhrmann, E., Scholz, I., Hess, W.R., and Graumann, P.L. (2007) Fluorescence staining of  
687 live cyanobacterial cells suggest non-stringent chromosome segregation and absence of a connection  
688 between cytoplasmic and thylakoid membranes. *BMC Cell Biol* **10**: 1–10.
- 689 Schwabe, G.H. (1960) Über den thermobionten Kosmopoliten *Mastigocladus laminosus* Cohn. *Hydrology*  
690 759–792.
- 691 Shih, P.M., Wu, D., Latifi, A., Axen, S.D., Fewer, D.P., Talla, E., *et al.* (2013) Improving the coverage of  
692 the cyanobacterial phylum using diversity-driven genome sequencing. *Proc Natl Acad Sci USA* **110**:  
693 1053–1058.
- 694 Singh, R.N., and Tiwari, D.N. (1969) Induction by Ultraviolet Irradiation of Mutation in the Blue-Green  
695 Alga *Nostoc linckia* (Roth) Born. et Flah. *Nature* **221**: 62–64.

- 696 Smith, D.J., Timonen, H.J., Jaffe, D. a, Griffin, D.W., Birmele, M.N., Perry, K.D., *et al.* (2013)  
697 Intercontinental dispersal of bacteria and archaea by transpacific winds. *Appl Env Microbiol* **79**: 1134–  
698 1139.
- 699 Soe, K.M., Yokoyama, A., Yokoyama, J., and Hara, Y. (2011) Morphological and genetic diversity of the  
700 thermophilic cyanobacterium, *Mastigocladus laminosus* (Stigonematales, Cyanobacteria ) from Japan and  
701 Myanmar. *Phycol Res* **59**: 135–142.
- 702 Stevens, S.E.J., Nierzwicki-Bauer, S.A., and Balkwill, D.L. (1985) Effect of nitrogen starvation on the  
703 morphology and ultrastructure of the cyanobacterium *Mastigocladus laminosus*. *J Bacteriol* **161**: 1215–8.
- 704 Szklarczyk, R., and Heringa, J. (2004) Tracking repeats using significance and transitivity. *Bioinformatics*  
705 **20**: 311–317.
- 706 Thurston, E.L., and Ingram, L.O. (1971) Morphology and fine structure of *Fischerella ambigua*. *J Phycol*  
707 **7**: 203–210.
- 708 Tomitani, A., Knoll, A.H., Cavanaugh, C.M., and Ohno, T. (2006) The evolutionary diversification of  
709 cyanobacteria: molecular-phylogenetic and paleontological perspectives. *Proc Natl Acad Sci USA* **103**:  
710 5442–5447.
- 711 Wildon, D.C., and Mercer, F. V (1963) The ultrastructure of the vegetative cell of blue-green algae. *Aust J*  
712 *Biol Sci* **16**: 585–596.
- 713 Wilk, L., Strauss, M., Rudolf, M., Nicolaisen, K., Flores, E., Kühlbrandt, W., and Schleiff, E. (2011)  
714 Outer membrane continuity and septosome formation between vegetative cells in the filaments of  
715 *Anabaena* sp . PCC 7120. *Cell Microbiol* **49**: 1–12.
- 716 Zhang, J.-Y., Chen, W.-L., and Zhang, C.-C. (2009) *hetR* and *patS* , two genes necessary for heterocyst  
717 pattern formation , are widespread in filamentous nonheterocyst-forming cyanobacteria. *Microbiology*  
718 **155**: 1418–1426.

719



**Table 1.** Exchange (E) and flux coefficients (F) for 5-CFDA in *M. laminosus*.

measurement	mean E [ $s^{-1}$ ] ( $\pm$ s.d.)	mean F [ $\mu m^3 s^{-1}$ ] ( $\pm$ s.d.)
1. cells in narrow trichomes	$0.159 \pm 0.072$	$7.65 \pm 5.19$
2. cells in wide trichomes	$0.058 \pm 0.044$	$3.60 \pm 2.47$
3. cells in hormogonia	$0.132 \pm 0.063$	$3.14 \pm 1.04$

t-tests indicate that E and F are significantly different in (1) and (2) ( $P < 0.00001$ ). Number of experiments performed for (1) 27, (2) 57, and (3) 9

## Figure Legends

FIG.1. Different types of branching in *M. laminosus*, and their development revealed by confocal (A,B,D) and transmission electron microscopy (C). Two main types of branching are present in *M. laminosus*, namely (reverse) “Y”- (A) and “T”-branching (B). While the division plane is localised parallel to the main filament axis in “T”-branching (B), it remains nearly transversal to the main filament axis during the formation of a (reverse) “Y”-branch (A,C). Cells at the terminus of the main trichome grow into the direction of the main filament but alter their cell shape (D). A,B. The images show FM1-43 FX fluorescence (yellow; left), chlorophyll *a* fluorescence (magenta, middle), and an overlay of both (right). Scale bars, 5 $\mu$ m. C. Electron micrograph of a thin section prepared with KMnO<sub>4</sub>; scale bar, 2 $\mu$ m. D. Bright-field image; scale bar, 5 $\mu$ m.

FIG. 2. Intercellular transfer of 5-CFDA between branch and main trichome in a “T”-branch of *M. laminosus*. A. FRAP image sequence. Only 5-CFDA fluorescence is shown. The left image was recorded prior to bleaching (pre). After bleaching out fluorescence in the branch (t = 0), the change in fluorescence intensity was followed over 32 s. Scale bars, 5  $\mu$ m. B. Quantitation of cell fluorescence of the FRAP sequence displayed in A. Regions of interest (ROI) were defined as shown in the left image, the “T”-branch comprised of three cells was considered as one ROI (“cell 3”). The corresponding fluorescence recovery is indicated in the right graph. Scale bar, 5  $\mu$ m.

FIG. 3. Electron micrographs of ultra thin sections through the septal region of *M. laminosus*, and localisation of SepJ by immunofluorescent labelling. A,B. Electron micrographs indicate the presence of structures connecting the cytoplasm of adjacent cells (septosomes; arrows) in *M.*

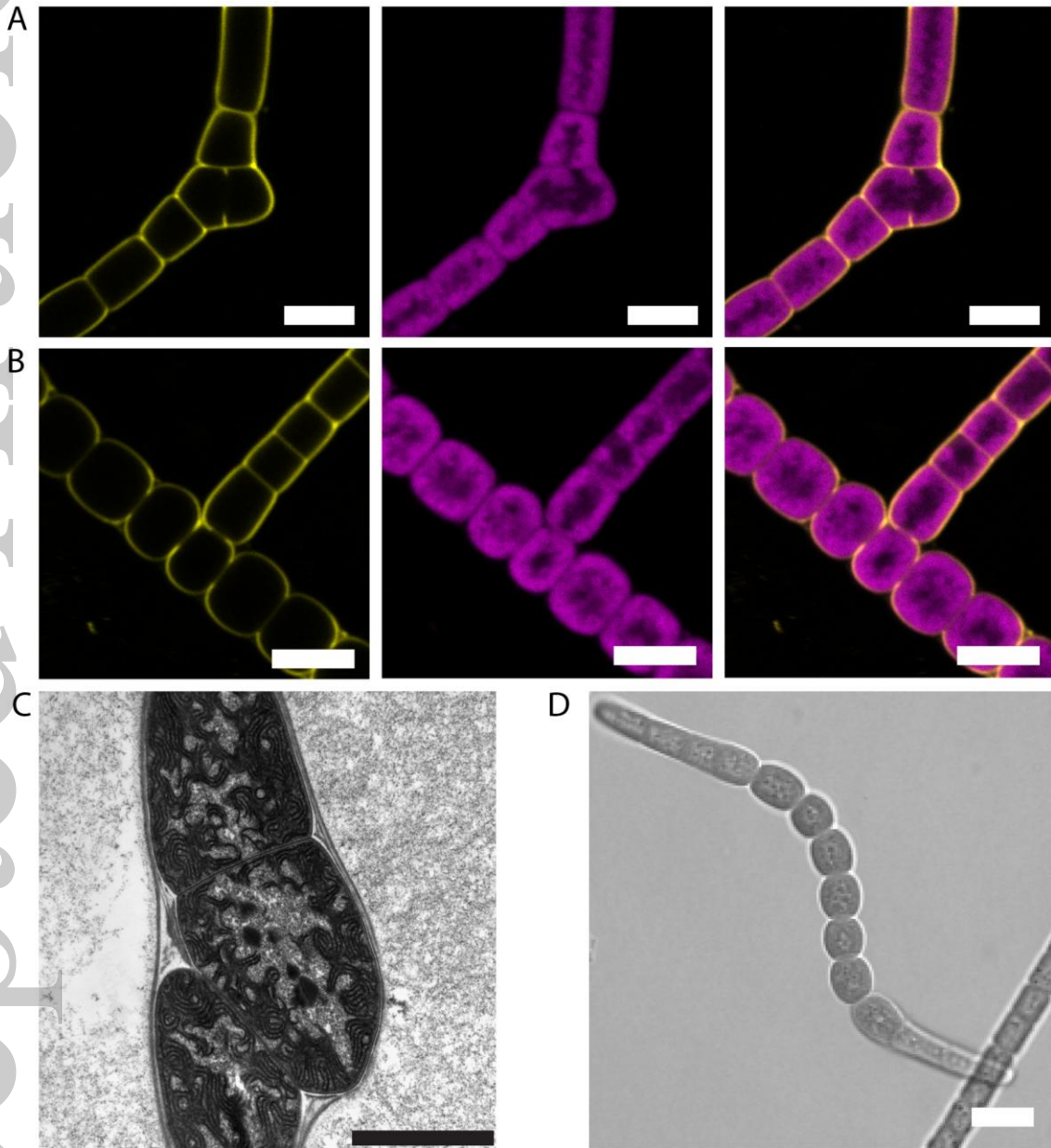
*laminosus*, using either a  $\text{KMnO}_4$ - (A) or a  $\text{OsO}_4$ -based preparation method (B). Septosomes are present between vegetative cells (A), and between vegetative cells and heterocysts (B). Note that the outer membrane does not enter the septum. CP – cyanophycin plug. Scale bars, 200nm. C. Localisation of SepJ in *M. laminosus* by immunofluorescent labelling. SepJ is localised in distinct spots in the septa between two adjacent vegetative cells. A branching point shows three distinct regions where SepJ is present (arrow). The images show SepJ immunolabelling (green; left), fluorescence of chlorophyll *a* (magenta; middle), and an overlay of both (right). Scale bars, 5 $\mu\text{m}$ .

FIG. 4. Position of heterocysts in filaments of *M. laminosus*. A-D. Heterocysts (arrows) can be found either in the branching start of “T”- (A) or (reverse) “Y”-branches (C), or in the new formed lateral branches (B and D, respectively). Note the position of cyanophycin granules in the heterocysts. They are always located close to cells they are connected with. Scale bars, 5  $\mu\text{m}$ . E. Double heterocyst in a narrow trichome of *M. laminosus* (arrows). Cyanophycin granules are located at each pole of the cell, resulting in two cyanophycin plugs between two heterocysts. Scale bar, 10  $\mu\text{m}$ . F. Electron micrograph of an ultra-thin section of a heterocyst in *M. laminosus*. A cyanophycin plug (CP) is present in the neck region. Rearrangements of thylakoid membranes are visible. The sample was prepared using the  $\text{KMnO}_4$  method. Scale bar, 1 $\mu\text{m}$ .

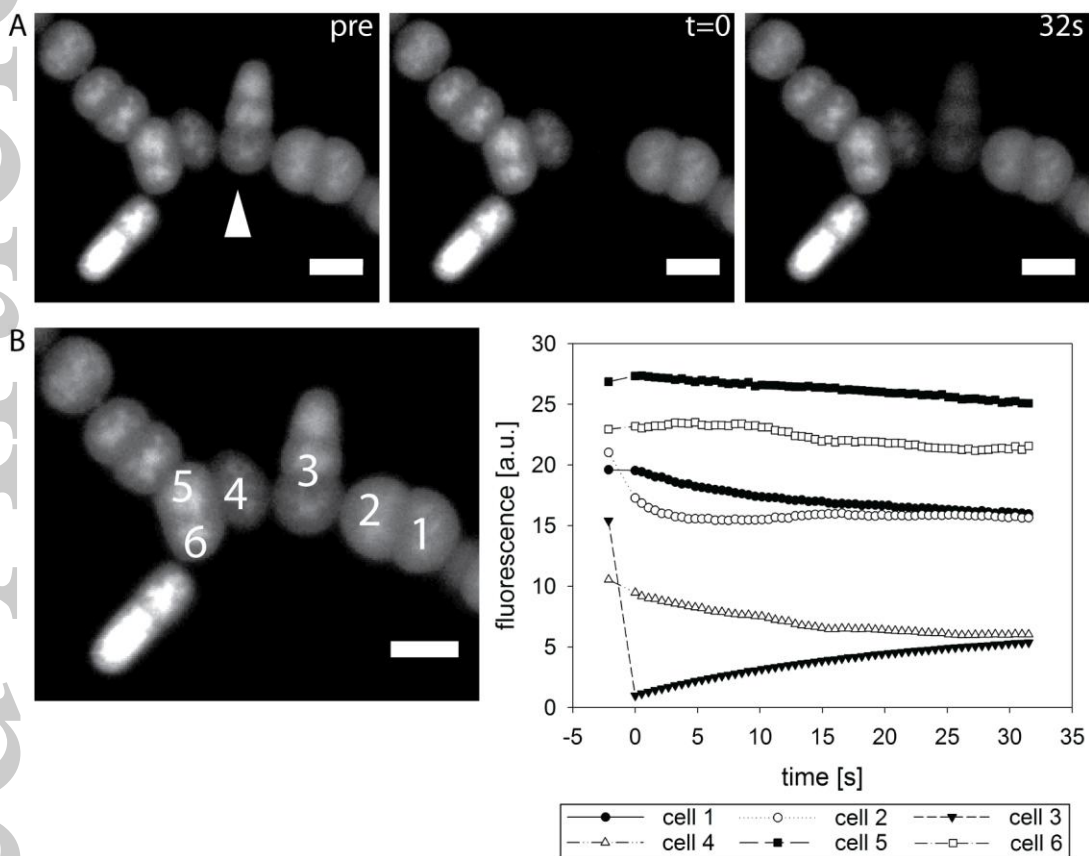
FIG. 5. Function of necridia in intercellular communication, and their localisation in filaments of *M. laminosus*. A. FRAP image sequence of 5-CFDA loaded cells. Intercellular transfer is inhibited between main trichome and branch by the formation necridium (grey arrow). The left image was recorded prior to bleaching (pre). After bleaching out fluorescence in the branch ( $t = 0$ ), recovery was followed over 24 s. The ROI is indicated with a white arrow. Scale bars, 5 $\mu\text{m}$ . B-D. Position of necridia and reorganisation of membranes in filaments of *M. laminosus*. Necridia

(arrows) can be found in the branching start (B), at the beginning of a recently formed branch (C), or at various positions within a narrow trichome (D). Their position follows no regular pattern. Two necridia can be even found in a single filament, separated only by one vegetative cell (D). The images show FM1-43 FX fluorescence (yellow; left), autofluorescence (magenta, middle) and an overlay of both (right). Scale bars, 5  $\mu\text{m}$ .

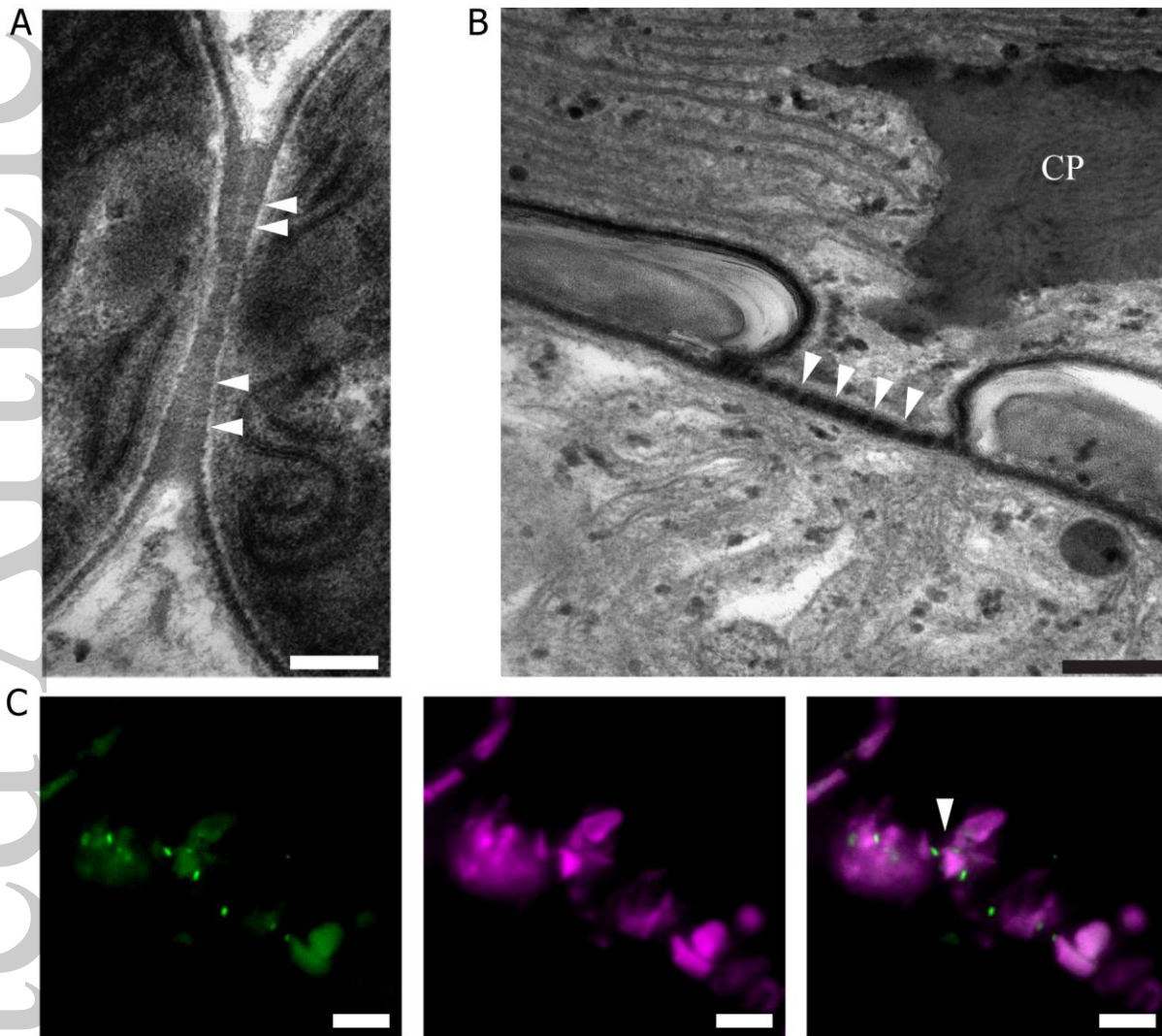
FIG. 6. Appearance of necridia after filament release. A. Localisation of DNA in a hormogonium of *M. laminosus*. DNA was visualised by staining cells with Hoechst 33258 (blue). Autofluorescence is shown in magenta. An overlay with the bright-field image illustrates the position of DNA in the hormogonium, while a dead part remains at the end of the released filament (arrow). Scale bars, 5  $\mu\text{m}$ . B. Electron micrograph of an ultra-thin section of a branch terminus after filament breakage via necridium formation. Note that plasma membrane (PM) and outer membrane (OM) are sealed at the terminal cell to prevent cell death by molecule efflux. The sample was prepared with the method based on  $\text{KMnO}_4$ . Scale bar, 1  $\mu\text{m}$ .



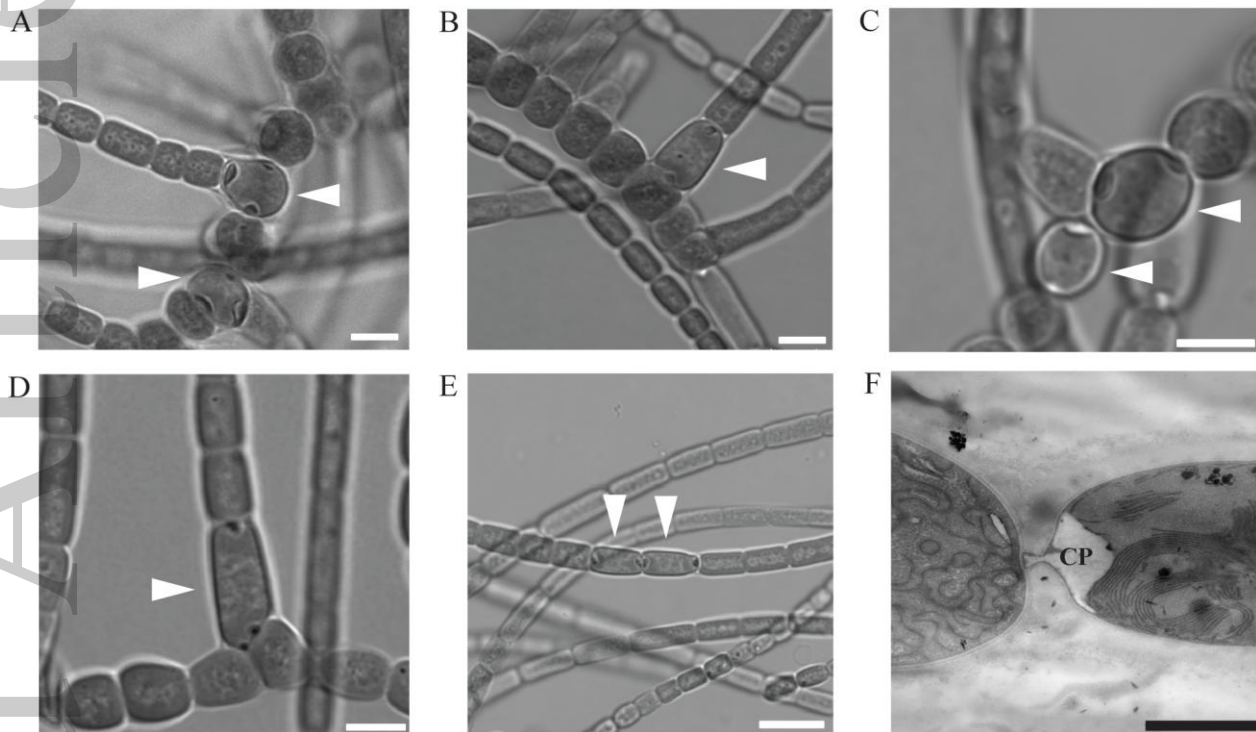
mmi\_12506\_f1



mmi\_12506\_f2

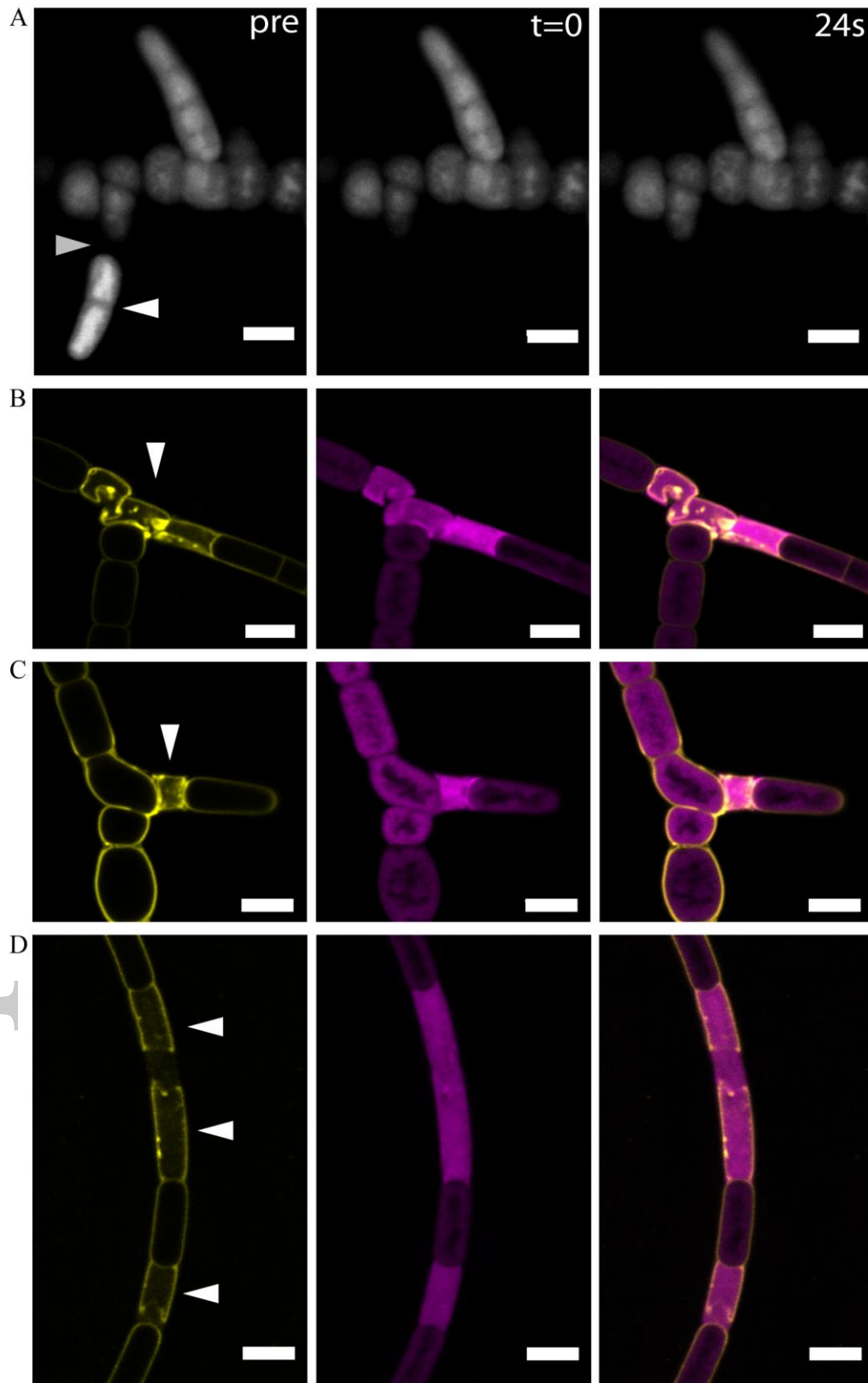


mmi\_12506\_f3

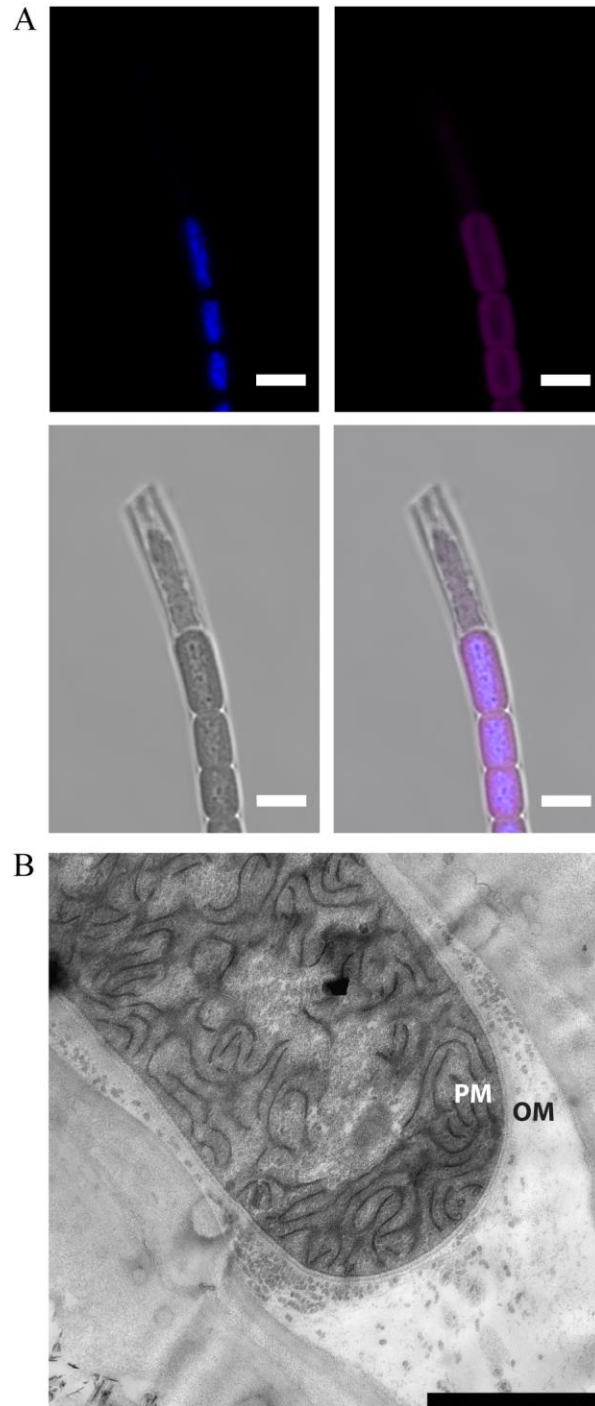


mmi\_12506\_f4





mmi\_12506\_f5



mmi\_12506\_f6